

See discussions, stats, and author profiles for this publication at: <https://www.researchgate.net/publication/26672179>

Natural Attenuation of Arsenic by Sediment Sorption and Oxidation

ARTICLE in ENVIRONMENTAL SCIENCE AND TECHNOLOGY · JULY 2009

Impact Factor: 5.33 · DOI: 10.1021/es802841x · Source: PubMed

CITATIONS

17

READS

13

3 AUTHORS, INCLUDING:



[Peggy A. O'Day](#)

University of California, Merced

90 PUBLICATIONS 2,399 CITATIONS

SEE PROFILE



[Janet Hering](#)

Eawag: Das Wasserforschungs-Institut des ...

128 PUBLICATIONS 6,074 CITATIONS

SEE PROFILE

Natural Attenuation of Arsenic by Sediment Sorption and Oxidation

SUNKYUNG CHOI,[†] PEGGY A. O'DAY,^{*,†}
AND JANET G. HERING^{‡,§}

School of Natural Sciences, University of California,
P.O. Box 2039, Merced, California 95344, and Department of
Environmental Science and Engineering, California Institute
of Technology, Pasadena, California 91125

Received October 7, 2008. Revised manuscript received
March 31, 2009. Accepted April 14, 2009.

Arsenic sorption onto aquifer sediments was investigated in anaerobic laboratory batch and column uptake experiments and characterized by As, Fe, and Mn X-ray absorption spectroscopy (XAS) to estimate the extent and mechanism of abiotic sorption and oxidation of As(III). Batch experiments at pH 6 showed that the amount of As(III) or As(V) sorption from synthetic background porewater to sediments was similar as a function of total As concentration, but slightly more As(V) was sorbed than As(III) with increasing As concentrations. Column experiments with As(III) solutions in the absence and presence of dissolved Fe²⁺ showed more As uptake in the presence of Fe but also more Fe desorption during flushout with As-free solutions such that net As uptake was similar to, or less than that of, the Fe-free experiment. Fits to bulk Fe X-ray absorption near-edge spectroscopy (XANES) spectra showed no change between unreacted and reacted sediments. Manganese XANES revealed small increases in absorption in the spectral region associated with Mn(II) after reaction, indicating sediment Mn reduction. However, XANES spectra showed that Mn is not present as Mn^{IV}O₂(s) but is probably substituted into other sediment minerals as a mixture of Mn(II,III). Quantitative analyses of As XANES spectra, which indicated mixtures of As(III) and As(V) after reaction with As(III) solutions, were used to estimate a fraction of As(V) in excess of native As(V) in the sediment (0.2 mmol kg⁻¹) that corresponds to sorbed As(III) oxidized to As(V). The spectroscopic and solution data indicate that the aquifer sediments have a limited abiotic capacity to oxidize As(III), which did not exceed 30% of the total amount of As sorbed and was estimated in the range of 0.025–0.4 mmol kg⁻¹ sediment. In the presence of dissolved Fe²⁺, the precipitation of Fe(III) hydrous oxide phases will be an effective mechanism for As scavenging only if there exists sufficient dissolved oxygen in groundwater to oxidize Fe. Once the aqueous oxidative capacity is exhausted, dissolved Fe²⁺ may compete with As(III) for the limited abiotic oxidation supplied by sediment Mn-bearing phases.

Introduction

Recent attention has focused on the mobilization of As from aquifer sediments as a source of groundwater contamination from either natural or anthropogenic activities that increase dissolved organic carbon, stimulate microbial processes, and generate reduced conditions. Laboratory and field studies have demonstrated that microbial reduction of As(V) and Fe(III) associated with reactive iron phases in sediments and coupled to the oxidation of organic carbon from either anthropogenic or natural sources is a likely mechanism for subsurface As mobilization (1–5). In addition to serving as an As source, however, aquifer sediments also act as a sink for dissolved As, which can be partitioned from aqueous to solid phases by sorption or (co)precipitation processes. The extent of As removal from groundwater by aquifer sediments depends on the mechanisms controlling the aqueous-solid partitioning, which are a function of porewater chemistry, pH, sediment chemistry, and groundwater flow conditions (6–9). The U.S. Environmental Protection Agency (EPA) has recently discussed the possible use of monitored natural attenuation (MNA) as a remediation approach for subsurface As because of its widespread occurrence at Superfund and other sites of contamination (10). Successful implementation of MNA and long-term viability requires knowledge of As sequestration mechanisms and factors that may influence release. As part of a comprehensive risk assessment and mitigation approach, MNA may provide a low-cost remedy at sites with appropriate biogeochemical characteristics and attenuation capacity (11, 12).

In this context, the mobilization and fate of naturally occurring As was examined at a field site where anaerobic bioremediation had been employed to treat a tetrachloro-ethene plume (13). At the former Fort Devens Reserve Forces Training Area (MA), groundwater is contaminated with chlorinated solvents originating in a 8100 m² source area from former fuel and solvent storage and use. Pilot testing of in situ remediation for chlorinated solvents was conducted in 2004–2005, in which almost 50000 gallons of 5–13% molasses solution was injected into the test area. Monitoring of groundwater wells downgradient of the injection showed that As was mobilized as reducing conditions were established from biodegradation processes. However, elevated arsenic concentrations were not detected further than about 30 m downgradient of the injection area, although estimated groundwater velocities predict much further migration, indicating that As sequestration was occurring by natural processes in the aquifer (13).

The aim of this study was to examine the mechanism and extent of arsenic uptake in laboratory batch and column experiments, using field sediments from cores taken at the Fort Devens site in order to quantify the ability of natural sediments to attenuate As. We explored the hypothesis that sediment-associated Mn(III,IV) may serve as a natural abiotic oxidant of sorbed As(III) to As(V), as proposed in prior studies (14–16). Other potential mechanisms of attenuation are sorption of As(III) to sediments without oxidation, or oxidation of dissolved Fe²⁺ and precipitation of Fe(III) hydroxide, with sorption or coprecipitation of As. The ability of sediments to sorb As(III) (as arsenite) and As(V) (as arsenate) from synthetic groundwater in the presence and absence of dissolved Fe²⁺ and quantification of the extent of sediment As oxidation in the sorbed fraction were examined by combining uptake from solution with X-ray absorption spectroscopic interrogation of oxidation state changes of As, Mn, and Fe.

* Corresponding author phone: (209) 228-4338; e-mail: poday@ucmerced.edu.

[†] University of California.

[‡] California Institute of Technology.

[§] Current address: Eawag, Swiss Federal Institute of Aquatic Science & Technology, Ueberlandstrasse 133, CH-8600 Duebendorf, Switzerland.

Experimental Section

Batch and Column Experiments. Batch experiments of arsenite [As(III)] and arsenate [As(V)] sorption and column experiments of As(III) sorption were done on a composite sediment from Fort Devens core SMW-3 (homogenized from depths of 39.6, 41.2, and 42.7 m). All experiments were done in an anaerobic glovebox with deoxygenated synthetic groundwater (DSG). For batch experiments, 1 g wet sediment was mixed with 20 mL synthetic groundwater with NaAsO_2 or Na_2HAsO_4 at total concentrations of 10^{-6} , 10^{-5} , 10^{-4} , or 10^{-3} M and equilibrated at ambient temperature in the dark for 24 h (in duplicate). A parallel set of samples was treated with 2% formaldehyde for microbial sterilization. After reaction, pH was measured, samples were centrifuged (pH checked after centrifugation), supernatant solutions were removed, and solution aliquots were either filtered (0.2 μm nylon) or left unfiltered. The remaining solid sediment was immediately double bagged in a N_2 atmosphere and frozen until XAS data collection (see Supporting Information for details).

Flow-through column experiments were conducted using a polypropylene (PPE) column (2.54 cm in diameter and 10.2 cm in height). A Spectra/Mesh filter was used at each end to avoid loss of particles during flow. To achieve uniform packing, we slurry packed the column with 82 g of sediment using DSG and then flushed it for 24 h with DSG at a constant flow rate (0.25 mL min^{-1} , 20 pore volumes d^{-1}). Bromide (Br^-) tracer tests were performed at three different flow rates and were similar in all cases (Supporting Information). Influent concentrations of 10^{-4} M As(III) with 2% formaldehyde were added to the influent DSG, and initial pH was adjusted to 6.1. One column was run with As(III) in unbuffered DSG, and two columns were run with As(III) and 10^{-3} M Fe(II) (as $\text{FeCl}_2 \cdot 4\text{H}_2\text{O}$), one with unbuffered DSG and one with a MES buffer (0.01 M, $\text{pK}_a \sim 6.1$). After column loading with As and Fe, influent solutions were switched to DSG only and flushed until effluent As concentration dropped to less than 5% of the original influent concentration ($C/C_0 < 0.05$). Transport parameters were determined by curve fitting of Br^- and measured breakthrough curves (Supporting Information). Effluent samples were collected, filtered through 0.2 μm nylon filters, and acidified with HNO_3 before analysis. After the column experiments, sediments were extruded from the columns in an anaerobic glovebox and separated into two sections (inlet end and outlet end). Each section was homogenized and kept frozen in a N_2 atmosphere until XAS data collection. For batch and column experiments, total As (filtered and unfiltered samples), Fe, and Mn were measured using inductively coupled plasma mass spectrometry (ICP-MS) (Agilent 7500cs), with detection limits of 0.2 ppb for As and Mn and 10 ppb for Fe. Sediment concentrations are reported on a dry weight basis (water content = 21.5%).

Synchrotron X-ray Absorption Spectroscopy (XAS). Composite sediment reacted in batch experiments with 10^{-5} , 10^{-4} , or 10^{-3} M total As(III) or As(V), and samples from column experiments with influent solutions of 10^{-4} M As(III) and 10^{-3} M Fe(II) were examined by X-ray absorption near edge spectroscopy (XANES) at the As, Fe, and Mn K-edges and were compared to the absorption spectra for each element of the unreacted composite sediment. Two As EXAFS spectra were collected on batch samples. In a N_2 atmosphere glovebox, samples for XAS were homogenized, and ~ 0.5 mg were ground to a fine powder, loaded into Teflon sample holders, sealed with Kapton tape, and quenched in liquid N_2 . Data were collected at the Stanford Synchrotron Radiation Lightsources (SSRL) on BL11-2 (3 GeV, 80–100 mA) with samples held at liquid He temperature (4–8 K). Fluorescence spectra were collected using a 30-element Ge solid state array detector. At each absorption edge, 3–12 successive scans were collected and averaged to obtain sufficient signal/noise.

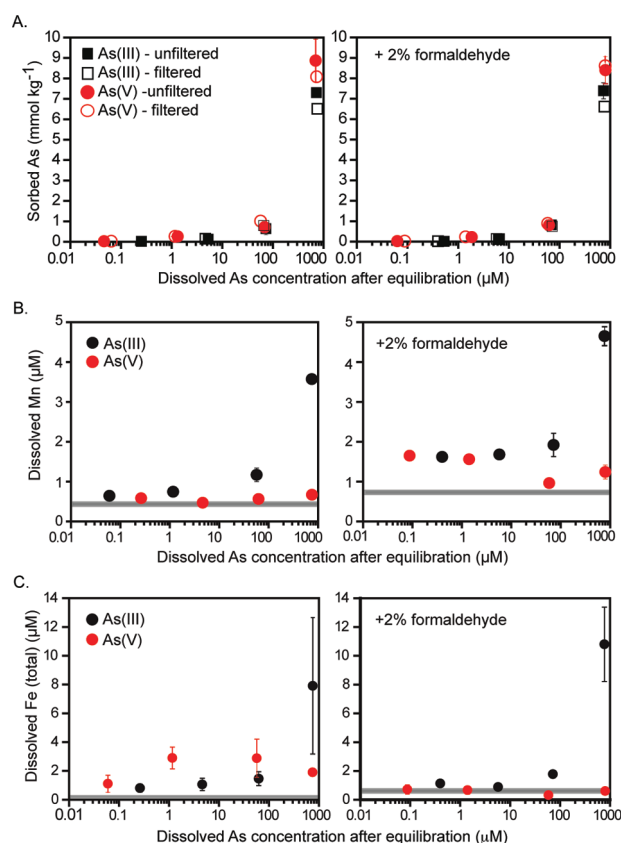


FIGURE 1. Batch sorption experiments with SMW-3 composite sediment reacted for 24 h in the dark with As(III) or As(V) solutions. (A) Arsenic uptake on sediment. (B) Dissolved Mn concentrations. (C) Dissolved Fe concentrations as a function of As concentration after reaction (filtered samples only for Mn and Fe). Gray bar is the average Mn or Fe concentration measured in solutions of control samples (sediment + solution with no As). Error bars from analyses of replicate samples are smaller than symbol if not shown.

No changes in oxidation states for As, Fe, and Mn were detected during XAS data collection. The SixPACK (17) and EXAFSPAK (18) software packages were used for data analysis, with previously analyzed reference spectra libraries (Supporting Information). Apparent fractions derived from XANES spectra were corrected to true fractions by fitting XANES of known mixtures for the end members and constructing a calibration curve. The observed As(III) and As(V) fractions from batch and column experiments were corrected to absolute fractions and normalized using the mixture calibration of Campbell et al. (19) for As(III) and As(V) sorbed to hydrous ferric oxide (HFO).

Results and Discussion

Batch and Column Experiments. Results of batch sorption experiments showed the amount of As(III) and As(V) sorption on sediments was similar as a function of total As concentration, but slightly more As(V) sorbed than As(III) at higher initial As concentrations (Figure 1A and Table SI-2 of the Supporting Information). With the exception of two As(III) samples, filtered and unfiltered solutions did not differ above analytical error. At the same initial As concentration, As uptake in samples sterilized with 2% formaldehyde did not differ significantly from untreated samples. Release of Mn to solution was small overall ($< 5 \mu\text{M}$), and near background levels at low total As concentrations (as indicated by As-free control samples). Dissolved Mn increased with higher total dissolved As(III) but remained low in all As(V) solutions (Figure 1B). Formaldehyde-treated samples showed slightly

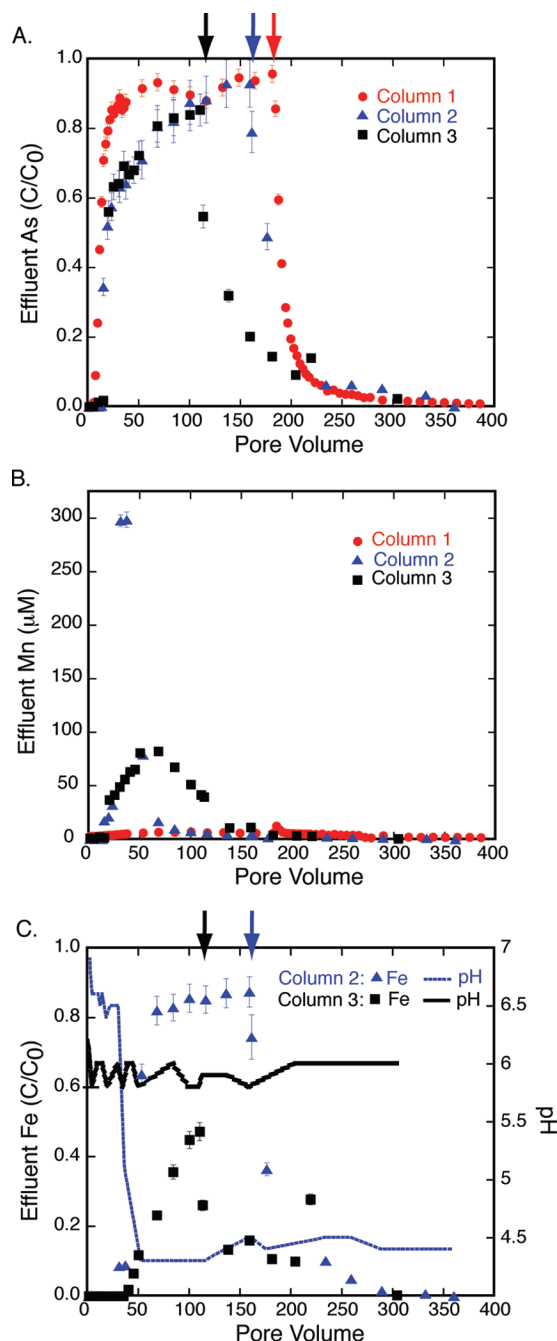


FIGURE 2. Effluent concentrations as a function of pore volume for column experiments. Column 1 is As(III) only. Column 2 is As(III) + Fe(II), unbuffered. Column 3 is As(III) + Fe(II), buffered. (A) Arsenic shown as concentration $C/\text{inlet concentration}, C_0 = 10^{-4} \text{ M As(III)}$. (B) Manganese. (C) Total Fe and pH, influent Fe concentration $C_0 = 10^{-3} \text{ M}$. Arrows indicate start of column flushout with As- and Fe-free background porewater solutions.

more Mn release ($\sim 1 \mu\text{M}$) than untreated samples at low total As concentrations. Dissolved Fe was slightly above background levels in unsterilized samples but near background levels in formaldehyde-treated samples, with an increase in Fe release in unsterilized and sterilized samples at the highest As(III) concentrations (Figure 1C).

In column experiments with As(III) solution (10^{-4} M) and no dissolved Fe (Column 1, Figure 2A), As breakthrough was slightly retarded compared to a conservative Br^- tracer (Figure SI-1 and Table SI-3 of the Supporting Information). Effluent As concentration was maximized ($C/C_0 > 0.9$) after ~ 25 pore volumes (PV) (Figure 2A). Column flush out with DSG started

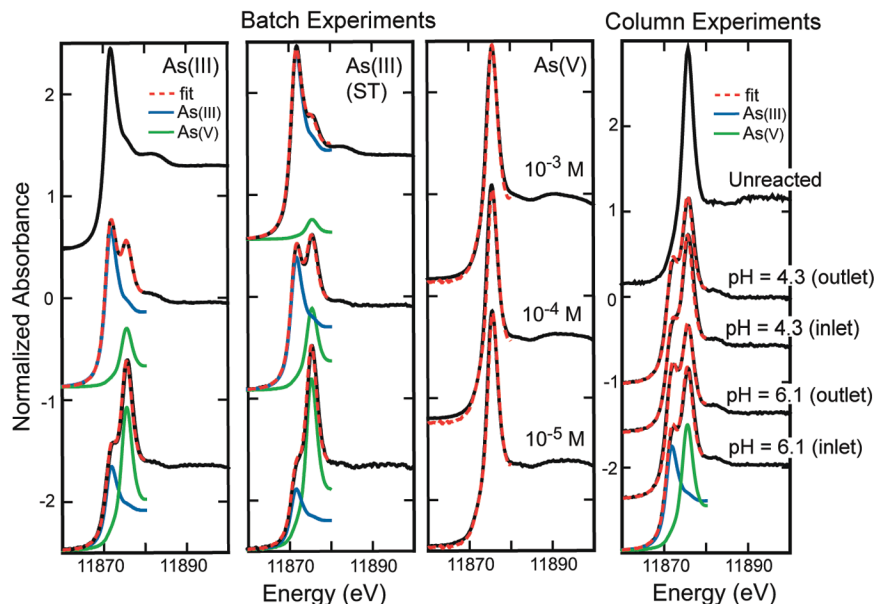
at 180 PV, and As concentrations decreased to $C/C_0 < 0.05$ after 54 PV of flushing. Measured effluent pH was ~ 6.5 to 25 PV and then decreased to pH ~ 6.2 – 6.3 and remained steady during flushout (data not shown). Effluent Mn was consistently low throughout As uptake and flushout in Column 1 (Figure 2B), which is in agreement with batch experiments. In column experiments in which $\text{Fe}^{2+}(\text{aq})$ was added to the influent solution, As breakthrough was more strongly retarded in the pH-unbuffered (Column 2) and pH-buffered (Column 3) experiments (Figure 2A). Column flushout, which was started in Column 3 (Figure 2A) before complete As or Fe breakthrough, was more dispersed than in Column 1 (Figure 2A). About 100 PV for Column 2 and more than 100 PV for Column 3 were flushed with DSG before As C/C_0 decreased to < 0.05 . Effluent Mn spiked in Column 2 (Figure 2B) during uptake of As at < 50 PV and then decreased sharply, corresponding to the drop in pH from ~ 6.5 to 4.3 in the unbuffered solution (Figures 2B and 2C). Effluent Mn was more dispersed in Column 3 (Figure 2B) during As uptake in the pH-buffered solution, and Mn release continued during initial flushout with DSG. Influent Fe concentrations did not reach complete breakthrough in either Column 2 or Column 3 (Figure 2C). In Column 2 (Figure 2C), effluent Fe maximized at $C/C_0 > 0.8$ when pH dropped from ~ 6.5 to 4.3, probably from precipitation or sorption of Fe. In pH-buffered Column 3 (Figure 2C) (pH ~ 6.1), Fe was strongly retarded and maximum C/C_0 was < 0.6 . Effluent Fe concentrations during flushout were variable, with more than 100 PV of DSG flushed before C/C_0 decreased to < 0.05 .

Calculation of As uptake and release in column experiments showed that As breakthrough was more strongly retarded, and that more As was initially sorbed, in Columns 2 and 3 compared with Column 1 (Table SI-4 of the Supporting Information). However, Columns 2 and 3 also had more As desorption such that net As retention by the sediment (total sorbed – total desorbed) was lowest in Column 3 and similar in Columns 1 and 2 (Table SI-4 of the Supporting Information). Influent Fe was retained in Column 2 (60%), where pH decreased from 6.5 to 4.3 during flushout, and in Column 3 (69%), buffered at pH 6.1 (Table SI-4 of the Supporting Information). About 4–5 times more Mn was released from sediments in Columns 2 and 3 in the presence of dissolved Fe than in Column 1 with no Fe (Table SI-4 of the Supporting Information).

Synchrotron X-ray Characterizations. The As XANES spectrum of the unreacted SMW-3 composite sample showed that all native As in the sediment was present as As(V). Batch sediments reacted with As(V) solutions at different initial concentrations retained their As(V) speciation after sorption, as indicated by the characteristic X-ray absorption maximum at $\sim 11875 \text{ eV}$ (Figure 3). Sediments reacted with As(III) solutions in batch and column experiments showed mixtures of As(V) and As(III), indicated by the characteristic As(III) maximum absorption at 11872 – 11873 eV . The relative proportions of As(III) and As(V) in reacted sediments were quantified by linear combination fits of the XANES spectra. As shown in Table 1, the fraction of As(III) relative to As(V) determined by XANES increased with increasing As(III) concentration in solution in batch experiments, which is consistent with As(III) sorption on sediments with native As(V). In column experiments, the fraction of As(III) in sediments determined by XANES fits at the end of the experiment varied from 43–58% of total As. Quantitative fits of two EXAFS spectra of sediment reacted in batch experiments with As(III) or As(V) confirmed adsorption of As as the mechanism of uptake (Supporting Information).

For sediments reacted with As(III), Fe and Mn XANES spectra of bulk sediments were examined to assess changes in oxidation state relative to the unreacted sediment. Comparison of unreacted and reacted Fe XANES showed no

A. Arsenic XANES



B. Mn XANES

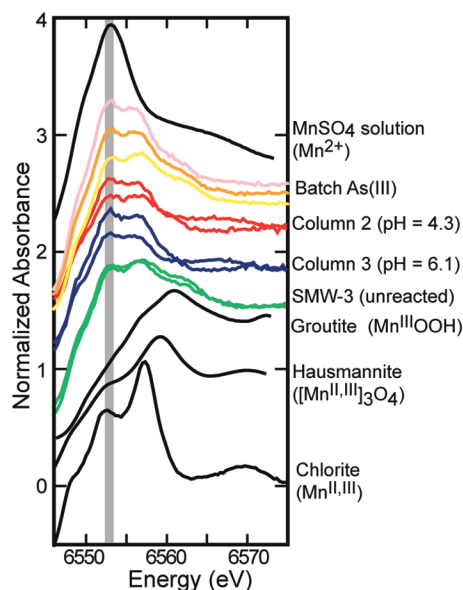


FIGURE 3. (A) Normalized As XANES spectra and quantitative fit deconvolutions with reference As(III) (blue) and As(V) (green) spectra (Table 1) for batch sediments reacted with As(III) or As(V) solutions (10^{-3} , 10^{-4} , and 10^{-5} M) and column sediments reacted with 10^{-4} M As(III) and 10^{-3} M Fe(II) solutions. Column 2 is pH 4.3, and Column 3 is pH 6.1. ST are samples sterilized with 2% formaldehyde. (B) Normalized Mn XANES spectra of batch (pink is 10^{-4} M, orange is 10^{-5} M, and yellow is 10^{-3} M) and column sediments (inlet and outlet ends) and two unreacted SMW-3 sediments (composite and 43 m depth). Reference spectra (black lines) are 10 mM $\text{Mn}^{2+}\text{SO}_4$ solution, natural groutite ($\alpha\text{-MnOOH}$), natural hausmannite ($\alpha\text{-Mn}_3\text{O}_4$), and natural Fe-chlorite (ripidolite, CCa-2) from the Clay Mineral Society Source Clays Repository with 0.1% MnO. Shaded bar indicates the spectral region generally associated with reduced Mn(II).

to very minor changes in spectral features (Figure SI-3 of the Supporting Information). Quantitative least-squares fits of sediment Fe XANES, using mineral reference compounds, showed that sediment Fe was a mixture of mica (represented by illite), chlorite, and magnetite, in approximately the same proportions ($\sim 50:30:20$) in all batch and columns experiments and in the unreacted sediment (Table SI-6 of the Supporting Information). Small changes in Fe oxidation state (<5 mol % of total Fe) would be difficult to detect in bulk XANES spectra. In column experiments with influent $\text{Fe}^{2+}(\text{aq})$, calculation of net Fe retention indicated that the fraction of sorbed Fe was small ($8\text{--}12$ mmol kg^{-1}) compared to the total Fe originally present in the sediment (1.39 wt % or 249 mmol

kg^{-1}) such that precipitation of Fe(III) in the column or sorption of Fe(II) was not detected in bulk XANES spectra.

Comparison of Mn XANES spectra between unreacted sediment and As(III)-reacted batch experiments showed some spectral differences (Figure 3B). The unreacted spectra could not be fit with mixtures of pure Mn compounds. Qualitative comparisons with reference compounds suggest a mixture of mostly Mn(II,III) oxidation states in solid phases that might be associated with magnetite, chlorite, or other phyllosilicate phases. Sediment Mn was not predominantly associated with pure $\text{Mn}^{\text{IV}}\text{O}_2$ phases, which have maximum X-ray absorption edges at higher energies ($\sim 6562\text{--}6564$ eV) than those observed in the sediments (20, 21). In batch

TABLE 1. Arsenic XANES Fits, Corrected XANES, and Estimated Fractions of Sorbed As(III) Oxidized to As(V) from XANES Fits

sample ^a	component	fitted XANES fraction ^b	total	corrected XANES fraction ^c	sorbed As ^d (mmol kg ⁻¹)	excess As(V) ^e (mmol kg ⁻¹)	excess As(V) (% As sorbed)
batch experiments: As(III)							
10 ⁻³ M	As(III)	0.96	0.96	1.0	6.51	n.o.	n.o.
10 ⁻³ M (ST)	As(III)	0.93	1.01	0.92	7.39	0.40	5
	As(V)	0.08		0.08			
10 ⁻⁴ M	As(III)	0.78	1.03	0.70	0.789	0.078	10
	As(V)	0.25		0.30			
	As(III)	0.66	1.01	0.59	0.749	0.15	20
10 ⁻⁴ M (ST)	As(V)	0.35		0.41			
10 ⁻⁵ M	As(III)	0.41	1.02	0.25	0.146	0.025	17
	As(V)	0.61		0.75			
10 ⁻⁵ M (ST)	As(III)	0.30	1.02	0.13	0.134	0.037	27
	As(V)	0.72		0.87			
batch experiments: As(V)							
10 ⁻³ M	As(V)	1.02	1.02		8.08		
10 ⁻⁴ M	As(V)	1.01	1.02		1.01		
10 ⁻⁵ M	As(V)	1.01	1.01		0.265		
Column 2 (pH 4.3) and Column 3 (pH 6.1): 10 ⁻⁴ M As(III) and 10 ⁻³ M Fe(II) (ST)							
pH 4.3 Outlet	As(III)	0.51	1.05	0.38	0.222 ^f	0.033	15
	As(V)	0.54		0.62			
	As(III)	0.43	1.05	0.25	0.222 ^f	0.062	28
pH 4.3 inlet	As(V)	0.62		0.75			
	As(III)	0.58	1.04	0.49	0.146 ^f	n.o.	n.o.
pH 6.1 outlet	As(V)	0.46		0.51			
pH 6.1 inlet	As(III)	0.51	1.04	0.38	0.146 ^f	0.0064	4

^a ST is sterilized with the addition of 2% formaldehyde. ^b Energy shifts for all fits were less than ± 0.18 eV. ^c Observed XANES fractions are corrected using the standard calibration reported in Campbell et al. (19) and normalized. ^d Calculated by difference from analysis of filtered aqueous samples (see Supporting Information for complete analyses). Native As(V) = 0.2 mmol kg⁻¹. ^e Estimated from $f_{\text{native As(V)}} = (m_{\text{native As(V)}})/(m_{\text{native As(V)}} + m_{\text{As(III) sorbed}})$; Excess As(V) = $f_{\text{XANES As(V)}} - f_{\text{native As(V)}}$; ^f is a fraction, and m is mass (per kg sediment dry wt). n.o. is not observed. ^f Net As uptake from integration of column data (Figure 2 and Supporting Information).

samples reacted with As(III) solutions at high concentration, Mn XANES spectra showed a shift in the amplitude of the absorption maxima at ~ 6553 and ~ 6557 eV, with the lower energy maximum increasing and the higher energy maximum decreasing, compared to those of the unreacted spectra (Figure 3B). Increasing absorption at lower energy and decreasing absorption at higher energy indicated a shift in the relative proportions of reduced Mn(II) to oxidized Mn(III,IV) species in the bulk sample (20, 22). This shift was less apparent in column-reacted sediments, but a slight increase in the absorption maximum at lower energy was observed.

Estimation of Sediment Oxidation of Sorbed As(III) from XANES Analysis. Normalized XANES spectra are sensitive to the proportions of the components present but not to the absolute amount of each. Furthermore, elements in different oxidation states have different absorption and fluorescence properties such that the apparent proportion derived from fitting XANES spectra does not necessarily equal the component fraction quantitatively (23–25). Corrected XANES fractions using a standard calibration (Table 1) give adjustments to the proportions of As(III) and As(V) of 0–18% compared to those of the uncorrected fits to account for these nonlinear effects.

The unreacted composite sediment contains 0.2 mmol kg⁻¹ native As by two different digestion methods (HF and HCl + HNO₃) (Supporting Information), all of which is present as As(V) as indicated by XANES. In batch reactions with As(V) solutions, native As and As(V) sorbed from solution remained as As(V). In batch and column experiments with As(III) solutions, the XANES spectra indicated a mixture of As(III) and As(V), of which a fraction is native As(V). On the basis of the amount of As(III) sorbed from solution and the known concentration of native As(V) in unreacted sediment, the fraction of sorbed As oxidized from As(III) to As(V) can be

estimated from the corrected XANES fractions by assuming no change in oxidation state or desorption of native As(V). Control experiments (Table SI-3 of the Supporting Information) and sequential extractions of SMW-3 sediment (13) indicated negligible desorption of sediment As in DSG and in the first extraction step targeting weakly adsorbed species, respectively. Thus, it is unlikely that sediment native As(V) was mobilized in batch experiments. In column experiments, release of As to solution was not observed in tracer experiments or in flushing of unreacted sediment with As-free DSG. Therefore, excess As(V), defined as the amount of As(III) sorbed and oxidized to As(V), was calculated from the total As(V) XANES fraction minus the native As(V) fraction (by mass). Table 1 shows the total amount of As(III) sorbed from solution, the calculated excess As(V) fraction, and the percent of As(III) oxidized to As(V) from this estimate. The largest uncertainty in the estimate, on the order of $\pm 5\%$ (25), arises from the error in XANES fits to mixtures of spectral components.

Although there is uncertainty and variability in the estimate, excess As(V) increased overall with increasing As(III) solution concentration and more As(III) sorption in batch experiments. With more sorption of As(III), the amount of excess As(V) is a decreasing percent of the total sorbed (Table 1). At 10⁻³ M As(III) (unsterilized), the sorbed As(III) fraction overwhelmed the signal from native and excess As(V) (Figure 3). In Columns 2 and 3 with As(III) and Fe²⁺(aq), the net amount of As retained after column flushout was 70–80% lower than in batch experiments at the same total As concentration (10⁻⁴ M) without dissolved Fe (Figure 3). The inlet end of the columns had a higher fraction of excess As(V) than that of the outlet end, suggesting a reaction front. Column 2 (flushout solution pH ~ 4.3) (Figure 3) had a high fraction of As(V) by XANES fits in inlet and outlet sections, and the inlet end had the highest percent of excess As(V),

even though the total concentration of excess As(V) (per kg sediment) was lower than in batch experiments at the same total As(III) concentrations. Column 3 (flushout solution pH ~6) had no excess As(V) in the outlet end and low excess As(V) in the inlet end (Table 1).

Arsenic Sorption, Sediment Speciation, and Environmental Implications. Analyses of As uptake behavior and XANES spectra of Fort Devens aquifer sediments provide a direct estimate of their ability to sorb As and potentially oxidize As(III) abiotically, and thus contribute to natural As attenuation. Experimental results presented here as well as observations from the field (13) indicate that sorption of As(III) and As(V) from solution is the dominant As attenuation mechanism. In batch experiments in the absence of $\text{Fe}^{2+}(\text{aq})$ at pH 6, As(V) sorption was similar to or slightly higher than As(III) sorption at the same total As concentration. For sorbed As(III), XANES spectra indicated that sediments have a limited but measurable capacity to oxidize sorbed As(III). Estimates (Table 1) suggest that this capacity varies from 0.025 to 0.4 mmol kg^{-1} (5–27% of total As(III) sorbed), compared with a native As(V) concentration of 0.2 mmol kg^{-1} . In experiments without $\text{Fe}^{2+}(\text{aq})$ at low total As(III) concentrations, estimated As(III) oxidation did not exceed 30% of the total amount sorbed and was lower than the amount of As(III) oxidized at higher As concentrations. This observation suggests that nonoxidative sorption sites may compete with sites where As(III) oxidation occurs, and therefore, abiotic oxidation of sorbed As(III) may be a relatively inefficient mechanism of As attenuation. The Fe-free column experiment (Column 1, Figure 2A), which was run for 8 days before flushout, showed slightly less total As sorption than batch experiments at the same concentration reacted for 24 h. Thus, there was no evidence for kinetic limitations to As sorption in the batch experiments.

In column experiments with $\text{Fe}^{2+}(\text{aq})$, As(III) uptake was higher than in the Fe-free column, but more As was desorbed during flushout with DSG such that net sorption was similar to or lower than that of the Fe-free experiment. In the column experiment with unbuffered DSG (Column 3) in which pH dropped to ~4.3, 15–28% (inlet and outlet) of the sorbed As(III) was oxidized to As(V), similar to that observed in batch experiments. In the pH 6 column, more Fe was retained on sediments than in the other columns, but little or no oxidation of sorbed As(III) to As(V) was observed (Table 1). Previous studies reported decreasing rates of As(III) oxidation with increasing pH from 4 to 7 with manganite (15) and aquifer materials (16), but there was also no effect with birnessite (14). Our observations may reflect competition between Fe and As(III) for sorption sites and possible blocking of oxidation sites because As(III) oxidation was observed in the Fe-free batch experiments at pH 6. Net retention of As by sediments is pH dependent and affected by competition for sorption sites from dissolved ions.

Spectroscopic evidence indicated a limited abiotic sediment oxidation capacity that may be associated with Mn-bearing phases. However, Mn is not present as $\text{Mn}^{\text{IV}}\text{O}_2(\text{s})$ and is probably substituted into silicate or oxide phases as a mixture of Mn(II, III) and possibly minor Mn(IV), oxidation states. Unlike the As K-edge, the energy of maximum X-ray absorption at the Mn K-edge is not strictly associated with specific oxidation states. Examination of Mn reference compound spectra shows that Mn absorption edges are variable and complex, with absorption following a general pattern from lower to higher oxidation state with increasing energy but with significant variability (20, 22, 23, 26). Qualitatively, the absorption shift to lower energy observed in the reacted sediments can be interpreted as a slight increase in the proportion of reduced Mn(II) in the sediments, suggesting a small amount of Mn reduction. In batch experiments, the molar amount of Mn released to solution

after reaction was much less than the amount of As sorbed, while in column experiments, more Mn was flushed from the columns than net As sorbed in the presence and absence of Fe. These observations point to pH-controlled sorption of Mn(II) produced by the oxidation of As or Fe as suggested in previous studies (14, 27).

Oxidation of dissolved Fe^{2+} and precipitation of Fe(III) (hydr)oxides are established mechanisms for increasing As sorption, either by supplying new sorption sites for As or by coprecipitating Fe(III) with As. In batch and column experiments, no obvious changes were observed in Fe XANES spectra that would indicate significant Fe(III) precipitation, although any precipitation was probably below detection in this system. This mechanism (abiotically or microbially mediated) consumes oxidative capacity within the aquifer and thus competes with other oxidation reactions. Oxidation of dissolved Fe^{2+} and precipitation can occur by consumption of porewater dissolved oxygen at the edges of an anaerobic plume or by sorption and oxidation of Fe(II) by sediment Mn oxides (20, 27). Spectroscopic evidence presented here showed that the sediments have a limited capacity to oxidize sorbed As(III) to As(V), but As sorption and oxidation will not necessarily provide better As attenuation at higher groundwater pH where As(V) desorption increases. The precipitation of Fe(III) hydrous oxide phases will be an effective mechanism for As scavenging only if there exists sufficient dissolved oxygen in groundwater to precipitate Fe(III). Once that oxidative capacity is exhausted, dissolved Fe^{2+} may compete with As(III) for the limited abiotic oxidation supplied by sediment Mn-bearing phases, which may be present in multiple Mn oxidation states.

Acknowledgments

This work was support by the U.S. Department of Defense, Strategic Environmental Research and Development Program (SERDP) Project ER-1374. N. Rivera, R. Root, and D. Beals assisted with data collection and analysis, and H.J. Reisinger and D.R. Burris provided field samples and support. Portions of this research were carried out at the Stanford Synchrotron Radiation Lightsource, a national user facility operated by Stanford University on behalf of the U.S. Department of Energy, Office of Basic Energy Sciences.

Supporting Information Available

Experimental details, sediment characterization, XAS analysis, tabulated data for batch and column experiments, results of As EXAFS fits, Fe XANES spectra and fit results. This information is available free of charge via the Internet at <http://pubs.acs.org>.

Literature Cited

- (1) Cummings, D. E.; Caccavo, F., Jr.; Fendorf, S. E.; Rosenzweig, R. F. Arsenic mobilization by the dissimilatory Fe(III)-reducing bacterium *Shewanella alga* BrY. *Environ. Sci. Technol.* **1999**, *33*, 723–729.
- (2) Ahmann, D.; Krumholz, L. R.; Lovley, D. R.; Morel, F. M. M. Microbial mobilization of arsenic from sediments of the Aberjona watershed. *Environ. Sci. Technol.* **1997**, *31*, 2923–2930.
- (3) Oremland, R. S.; Newman, D. K.; Kail, B. W.; Stolz, J. F. Bacterial Respiration of Arsenate and Its Significance in the Environment. In *Environmental Chemistry of Arsenic*; Frankenberger, W. T., Jr. Ed., Marcel Dekker, Inc.: New York, 2002; pp 273–295.
- (4) Inskeep, W. P.; McDermott, T. R.; Fendorf, S. Arsenic (V)/(III) Cycling in Soils and Natural Waters: Chemical and Microbiological Processes. In *Environmental Chemistry of Arsenic*; Frankenberger, W. T., Jr. Ed., Marcel Dekker, Inc.: New York, 2002; pp 183–215.
- (5) Cummings, D. E.; Snoeyenbos-West, O. L.; Newby, D. T.; Niggemeyer, A. M.; Lovley, D. R.; Achenbach, L. A.; Rosenzweig, R. F. Diversity of geobacteraceae species inhabiting metal-polluted freshwater lake sediments ascertained by 16S rDNA analyses. *Microbial Ecol.* **2003**, *46* (2), 257–269.

- (6) Welch, A. H.; Westjohn, D. B.; Helsel, D. R.; Wanty, R. B. Arsenic in the groundwater of the United States: Occurrence and geochemistry. *Ground Water* **2000**, *38*, 589–604.
- (7) Stollenwerk, K. G. Geochemical Processes Controlling Transport of Arsenic in Groundwater: A review of adsorption. In *Arsenic in Goundwater*; Welch, A. H., Stollenwerk, K. G. Eds.; Kluwer Academic Publishers: Boston, MA, 2003; pp 67–100.
- (8) Smedley, P. L.; Kinniburgh, D. G. A review of the source, behavior and distribution of arsenic in natural waters. *Appl. Geochem.* **2002**, *17* (5), 517–568.
- (9) McMahon, P. B.; Chapelle, F. H. Redox processes and water quality of selected principal aquifer systems. *Ground Water* **2008**, *46* (2), 259–271.
- (10) *Monitored Natural Attenuation of Inorganic Contaminants in Ground Water*; U.S. Environmental Protection Agency: Washington, DC, 2007; Vols. 1 and 2.
- (11) Reisinger, H. J.; Burris, D. R.; Hering, J. G. Remediating subsurface arsenic contamination with monitored natural attenuation. *Environ. Sci. Technol.* **2005**, *39* (22), 458A–464A.
- (12) Hering, J. G.; O'Day, P. A.; Ford, R. G.; He, Y. T.; Bilgin, A.; Reisinger, H. J.; Burris, D. R. MNA as a remedy for arsenic mobilized by anthropogenic inputs of organic carbon. *Ground Water Monit. Rem.*, unpublished work.
- (13) He, Y. T.; Fitzmaurice, A. G.; Bilgin, A.; Choi, S.; O'Day, P. A.; Horst, J.; Harrington, J.; Burris, D.; Hering, J. G. Geochemical processes controlling arsenic mobility in groundwater: A case study of arsenic mobilization and natural attenuation. *Appl. Geochem.*, unpublished work.
- (14) Scott, M. J.; Morgan, J. J. Reactions at oxide surfaces. 1. Oxidation of As(III) by synthetic birnessite. *Environ. Sci. Technol.* **1995**, *29*, 1898–1905.
- (15) Chiu, V. Q.; Hering, J. G. Arsenic adsorption and oxidation at Manganite surfaces. 1. Method for simultaneous determination of adsorbed and dissolved arsenic species. *Environ. Sci. Technol.* **2000**, *34* (10), 2029–2034.
- (16) Amirbahman, A.; Kent, D. B.; Curtis, G. P.; Davis, J. A. Kinetics of sorption and abiotic oxidation of arsenic(III) by aquifer materials. *Geochim. Cosmochim. Acta* **2006**, *70* (3), 533–547.
- (17) Webb, S. M. SixPACK: Sam's Interface for XAS Package. <http://www-ssrl.slac.stanford.edu/~swebb/sixpack.htm>, 2002.
- (18) George, G. N.; Pickering, I. J. *EXAFSPAK: A Suite of Computer Programs for Analysis of X-ray Absorption Spectra*; Stanford Synchrotron Radiation Laboratory: Menlo Park, CA, 2000.
- (19) Campbell, K. M.; Root, R. A.; O'Day, P. A.; Hering, J. G. A gel probe equilibrium sampler for measuring arsenic porewater profiles and sorption gradients in sediments: I. Laboratory development. *Environ. Sci. Technol.* **2008**, *42* (2), 497–503.
- (20) Villinski, J. E.; O'Day, P. A.; Corley, T. L.; Conklin, M. H. In situ spectroscopic and solution analyses of the reductive dissolution of MnO₂ by Fe(II). *Environ. Sci. Technol.* **2001**, *35* (6), 1157–1163.
- (21) Villalobos, M.; Lanson, B.; Manceau, A.; Toner, B.; Sposito, G. Structural model for the biogenic Mn oxide produced by *Pseudomonas putida*. *Am. Mineral.* **2006**, *91* (4), 489–502.
- (22) Tournassat, C.; Charlet, L.; Bosbach, D.; Manceau, A. Arsenic(III) oxidation by birnessite and precipitation of manganese(II) arsenate. *Environ. Sci. Technol.* **2002**, *36* (3), 493–500.
- (23) Ressler, T.; Wong, J.; Roos, J.; Smith, I. L. Quantitative speciation of Mn-bearing particulates emitted from autos burning (methylcyclopentadienyl) manganese tricarbonyl-added gasolines using XANES spectroscopy. *Environ. Sci. Technol.* **2000**, *34*, 950–958.
- (24) Zavarin, M.; Doner, H. E. Interpretation of heterogeneity effects in synchrotron X-ray fluorescence microprobe data. *Geochem. Trans.* **2002**, *3*, 51–55.
- (25) O'Day, P. A.; Rivera, N.; Root, R.; Carroll, S. A. X-ray absorption spectroscopic study of iron reference compounds for the analysis of natural sediments. *Am. Mineral.* **2004**, *89* (4), 572–585.
- (26) Bargar, J. R.; Tebo, B. M.; Villinski, J. E. In situ characterization of Mn(II) oxidation by spores of the marine *Bacillus* sp strain SG-1. *Geochim. Cosmochim. Acta* **2000**, *64*, 2775–2778.
- (27) Postma, D.; Appelo, C. A. J. Reduction of Mn-oxides by ferrous iron in a flow system: Column experiment and reactive transport modeling. *Geochim. Cosmochim. Acta* **2000**, *64* (7), 1237–1247.

ES802841X